Numerical Studies of Rossby Waves Using Finite Difference Methods

Astrid Bragstad Gjelsvik and Erlend Andreas Longva*
Department of Physics, University of Oslo, P.O. Box 1048 Blindern, N-0316 Oslo, Norway

In this project we study the behavior and evolution of Rossby waves in one and two spatial dimensions. The Rossby waves are described by a partial differential equation, which we solve using both forward and centered finite difference methods and Jacobi's method. We found the centered-time-centered-space (CTCS) method to be stable for $\Delta t \leq \Delta x$. The Rossby wave equation was solved using both sine waves and centered Gaussians as initial stream functions, and the simulations were done in both a periodic and a bounded domain. We reproduced the expected behavior for the wave propagation in the westward direction in all domains and in both one and two dimensions. The phase speed was found to be $|c| \simeq 0.00625$ with a relative error of 0.0128 for an initial sine wave in a periodic domain (1D).

I. INTRODUCTION

To understand the Earth system and the climate we experience, it is fundamental to describe large-scale fluid motion and flow, both in the atmosphere and in the ocean. Rossby waves are one of the phenomena we see in both the air and the sea, for example in the meandering nature of the atmospheric Jet Stream [6]. These waves were first identified by the Swedish-American meteorologist Carl-Gustaf Rossby [10]. Today they are believed to be very important in determining weather conditions around the globe, as their large-scale, slow-moving motion can transport heat between the tropics and the poles, determine storm tracks, and contribute to high tides and flooding in the ocean [8].

In this project we consider idealized representations of planetary Rossby waves. We implement boundary conditions representing both the ocean and the atmosphere. We set up the barotropic Rossby wave equation and solve it using different finite difference methods for partial differential equations. In doing so we make a comparison between the stability of different methods. The algorithms we implement are not only applicable to Rossby waves, but to a wide range of phenomena in nature that can be described using wave equations.

The content that follows is a presentation of the methods and theory we have used in the section "Method", followed by a presentation of our main findings in "Results". After this we discuss our findings in "Discussion", and finally conclude with a consideration of further prospects.

II. METHOD

In this section we first present the Rossby equation and where it comes from. We then find some analytical solutions for the Rossby equation in one dimension, and corresponding phase speeds. Afterwards we present how we discretize the Rossby equation and the algorithms we use to solve it numerically in both one and two spatial dimensions. Lastly we present the initial conditions we use and how we implemented our algorithms.

For all program code, tests runs, output files and results obtained see our GitHub-repository.

A. The Rossby wave equation

Rossby waves are planetary waves that result from the effect of Earth's rotation, or the Coriolis acceleration. The Coriolis parameter f varies with latitude and can be described as

$$f = 2\Omega \sin(\theta), \tag{1}$$

where $\Omega = 2\pi/\text{day}$ denotes the rotation of the Earth and θ is the latitude. The meridional variation can be approximated as a linear function, centered on a latitude θ_0, in the following way:

$$f \approx f_0 + \beta y. \tag{2}$$

Here $f_0 = 2\Omega \sin(\theta_0)$, $y = R_e(\theta - \theta_0)$ (R_e being the earths radius), and $\beta = \frac{\partial f}{\partial y}\Big|_{\theta_0} = 2\Omega\cos(\theta_0)/R_e$. This is called the β-plane approximation.

To describe flow in the atmosphere and oceans, we introduce the Coriolis acceleration into the Navier-Stokes equations as an acceleration which works perpendicular to the velocity $\mathbf{u}$ of the fluid. We assume the fluid to be incompressible, which allows us to express the velocity field $\mathbf{u}$ in terms of a streamfunction ψ. As a way of simplifying the problem, we use the shallow water equations. This approximation can be used when we are looking at fluid dynamics with large horizontal scales and small vertical scales, and therefore assume that the flow is primarily horizontal and does not vary significantly with height [7]. This makes it possible to integrate over depth so that we remove the vertical velocity from the equations. We can then obtain the conservation law

$$\frac{\mathrm{D}}{\mathrm{D}t}\frac{\zeta + f}{h} = 0, \tag{3}$$

* astridbg@student.matnat.uio.no
e.a.longva@fys.uio.no

which is the conservation of potential vorticity. The potential vorticity consists of the vorticity of the fluid column $\zeta = \nabla_H \times \mathbf{u}$ and the Coriolis parameter f, divided by the depth of the water column h. The conservation of potential vorticity tells us that a fluid column moving meridionally will have a change in vorticity due to the variation of f, which is the basis for the occurrence of Rossby waves. Linearising equation (3), assuming no bottom topography (constant h) and no mean flow, we can apply the β-plane approximation and get

$$\frac{\partial \zeta}{\partial t} + \beta v = 0 \tag{4}$$

where v is the meridional velocity perturbation. This equation can be written in terms of the streamfunction ψ, which is defined by $v = \frac{\partial \psi}{\partial x}$ and $u = -\frac{\partial \psi}{\partial y}$, yielding $\zeta = \nabla_H^2 \psi$. Equation (4) then becomes

$$\frac{\partial}{\partial t}\nabla_H^2 \psi + \beta \frac{\partial}{\partial x}\psi = 0 \tag{5}$$

which is what we know as the barotropic Rossby wave equation.

B. Analytical solutions

We use two possible analytical solutions to the Rossby wave equation in one dimension, one for periodic boundaries and one for solid boundaries. While the solid boundary solution representents flow in an ocean bounded by continents, the periodic boundary can represent the free-flowing atmosphere. We find the respective dispersion relations $\omega(k)$ and phase speeds c, which we compare with our numerical results. The phase speed of the wave is the speed at which the wave propagates in space, $c = \frac{\mathrm{d}x}{\mathrm{d}t}$. We can find it by considering the wavelength λ the wave travels over the period T, or $c = \lambda / T$. This is equivalent to the angular frequency ω over the wavenumber k, or $c = \omega / k$.

1. *Periodic boundaries*

A suitable wave solution for a periodic domain extending from $x = [0, L]$ (east-west) has the form

$$\psi = A\cos(kx - \omega t) \tag{6}$$

with $k = \frac{2n\pi}{L}$, $n = 1, 2, \ldots$. Here k is the wavenumber, ω is the frequency and A is the amplitude. Inserting this solution into equation (5) and solving for ω yields

$$\frac{\partial}{\partial t}\frac{\partial^2}{\partial x^2} A\cos(kx - \omega t) + \beta \frac{\partial}{\partial x} A\cos(kx - \omega t) = 0 \tag{7}$$

$$-\omega k^2 A\sin(kx - \omega t) - \beta k A \sin(kx - \omega t) = 0 \tag{8}$$

$$\omega = -\frac{\beta}{k} \tag{9}$$

which gives us the wave dispersion relation $\omega = -\beta L / 2n\pi$. We find the phase speed using the dispersion relation in equation (9), which gives

$$c = \frac{\omega}{k} = -\frac{\beta}{k^2} = -\frac{\beta L^2}{4n^2\pi^2}. \tag{10}$$

As the phase speed is negative, we see that the wave is propagating westward.

2. *Solid boundaries*

For the case with solid boundaries, we use a wave solution with the form

$$\psi = A(x)\cos(kx - \omega t). \tag{11}$$

Since there should not be any flow at the boundaries, we enforce this with Dirichlet boundary conditions $\psi = 0$ at $x = 0$ and $x = L$. Inserting this solution into equation (5) yields

$$\frac{\partial}{\partial t}\frac{\partial^2}{\partial x^2} A(x)\cos(kx - \omega t) + \beta \frac{\partial}{\partial x} A(x)\cos(kx - \omega t) = 0 \tag{12}$$

which results in the two equations

$$\frac{\partial A}{\partial x}(2\omega k + \beta) = 0 \tag{13}$$

$$\omega \frac{\partial^2 A}{\partial x^2} - \left(\omega k^2 + \beta k\right) A(x) = 0 \tag{14}$$

For full calculations, see section A 1 in the appendix. Equation (13) can be solved for ω, giving the dispersion relation

$$\omega = -\frac{\beta}{2k} \tag{15}$$

Inserting the above expression for ω into equation (14), we obtain the differential equation

$$\frac{\partial^2 A}{\partial x^2} + k^2 A(x) = 0 \tag{16}$$

which means that a suitable solution for $A(x)$ could be $B\sin(kx)$. Applying the Dirichlet boundary conditions, we find that $k = n\pi/L$, for $n = 1, 2, \ldots$, in other words k is quantized. Rossby waves with solid boundaries can in other words have the form

$$\psi = B\sin(kx)\cos(kx - \omega t) \tag{17}$$

where $k = \frac{n\pi}{L}$, $= 1, 2, \ldots$. The sine wave will be zero in the edges of the domain (or at more points, depending on the wave number), which means that it will "shape" the cosine wave that evolves in time. The phase speed is found to be

$$c = \frac{\omega}{k} = -\frac{\beta}{2k^2} = -\frac{\beta L^2}{2n^2\pi^2} \tag{18}$$

We see that the phase speed is half the speed of waves with periodic boundary conditions (provided that they have the same wavenumbers), and that the waves are still propagating westward.

C. Discretization and algorithm

We solve the Rossby waves equation numerically by discretizing equation (5), both in one and two spatial dimensions. We solve the equation by dividing it into two steps and scaling the equation to a non-dimensional form. The first step is to use the prognostic equation

$$\frac{\partial \hat{\zeta}}{\partial t} + \frac{\partial \hat{\psi}}{\partial x} = 0 \tag{19}$$

finding the scaled vorticity $\hat{\zeta}$ in the next time step, and then use the diagnostic equation

$$\nabla_H^2 \hat{\psi} = \hat{\zeta} \tag{20}$$

to find the time-corresponding scaled streamfunction $\hat{\psi}$. Equation (20) is Poisson's equation.

We approximate the derivates by finite differences. To do this, we use the following schemes

$$\frac{\partial \gamma}{\partial \rho} \approx \frac{\gamma_{i+1} - \gamma_i}{\Delta \rho} \tag{21}$$

$$\frac{\partial \gamma}{\partial \rho} \approx \frac{\gamma_{i+1} - \gamma_{i-1}}{2\Delta \rho} \tag{22}$$

$$\frac{\partial^2 \gamma}{\partial \rho^2} \approx \frac{\gamma_{i+1} - 2\gamma_i + \gamma_{i-1}}{\Delta \rho^2} \tag{23}$$

where γ is an arbitrary function, and ρ is an arbitrary variable discretized as $\rho_i = i\Delta\rho$. While equations (22) and (23) determine the derivate in point i by using the centered differences, equation (21) does so by using the forward difference. The forward difference scheme has a truncation error of $O(\Delta\rho)$, and the centered difference schemes have a truncation error of $O(\Delta\rho^2)$ [4].

We begin by applying these schemes to the 1 + 1 dimensional case, where x is our only spatial dimension and time t is the other one. The scaled spatial domain is $x \in [0, 1]$. We discretize time and space as

$$x_j = j\Delta x \tag{24}$$

$$t^n = n\Delta t \tag{25}$$

where Δx is the grid spacing and Δt is the time step. Using the forward differences scheme for the time stepping and centered differences for the spatial derivative, equation (20) becomes

$$\hat{\zeta}_j^{n+1} = \hat{\zeta}_j^n - \frac{\Delta t}{2\Delta x}(\hat{\psi}_{j+1}^n - \hat{\psi}_{j-1}^n) \tag{26}$$

Using centered differences for both time and space derivatives, on the other hand, we get

$$\hat{\zeta}_j^{n+1} = \hat{\zeta}_j^{n-1} - \frac{\Delta t}{\Delta x}(\hat{\psi}_{j+1}^n - \hat{\psi}_{j-1}^n) \tag{27}$$

While (26), also known as the forward-time-centered-space (FTCS) scheme, has a truncation error of $O(\Delta t) + O(\Delta x^2)$, equation (27) has a truncation error of $O(\Delta t^2) + O(\Delta x^2)$. Our wave problem is an instance of a hyperbolic partial differential equation, for which the FTCS is always unconditionaly unstable [1]. However, we can find a stability condition for (27), or the centered-time-centered-space (CTCS). This condition is also known as the Courant-Friedrich-Levy condition, and requires that the Courant number $C \leq 1$ [9]. In our case we have

$$C = \frac{\Delta t}{\Delta x} \Rightarrow \Delta t \leq \Delta x \tag{28}$$

The stability criterion for the CTCS scheme is that the time step is the same size as the grid space, or smaller.

The left hand side of equation (20) in one spatial dimension reduces to the second x-derivative of $\hat{\psi}$. We can therefore implement it as

$$\hat{\psi}_{j+1}^{n+1} - 2\hat{\psi}_j^{n+1} + \hat{\psi}_{j-1}^{n+1} = \Delta x^2 \hat{\zeta}_j^{n+1} \tag{29}$$

This is a set of linear equations that we can solve as a tridiagonal matrix problem.

For the case with solid boundary conditions, representing the (one-dimensional) ocean, we solve this set using a method based on Gaussian elimination where we precalculate the elements of the new off-diagonal matrix elements. We use forward substitution to find the elements on the right hand side of equation (29), and backward subsitution to find $\hat{\psi}$. This method is presented in our previous study of tridiagonal matrix problems [3]. We set the end points of $\hat{\psi}$ equal to zero.

For the case of periodic boundaries, representing the atmosphere, the tridiagonal matrix is however singular. We do therefore not employ Gaussian elimination, but the iterative Jacobi's method. This method is based on making guesses for the unknown $\hat{\psi}^{n+1}$, and iterating over it until it converges towards a certain value. We based this method on the work of Morten Hjort-Jensen [5]. We use modulo indexing as presented in our Ising model study [2] to get periodic boundaries.

Our algorithm for 1 + 1 dimensions thus becomes

```
initialise psi, zeta
for n = 0,..., T-1:
    for j = 0, ..., X:
        calculate zeta(j,n+1) using
        forward or centered
        differences scheme
    calculate psi(n+1) using
    Gaussian elimination or
    Jacobi's method
```

where `T` and `X` are the grid sizes for the time and space dimension respectively.

We expand our algorithm to the 2 + 1 dimensional case. This means that include the north-west spatial dimension y as well, which we discretize as

$$y_i = i\Delta y \tag{30}$$

Letting $\Delta y = \Delta x$, and $y \in [0,1]$, we can implement equation (20) as

$$\hat{\psi}_{i+1,j}^{n+1}+\hat{\psi}_{i,j+1}^{n+1}-4\hat{\psi}_{i,j}^{n+1}+\hat{\psi}_{i,j-1}^{n+1}+\hat{\psi}_{i-1,j}^{n+1} = \Delta x^2 \hat{\zeta}_{i,j}^{n+1} \quad (31)$$

using the scheme in equation (23) for both spatial dimensions. We solve this equation set using Jacobi's method. For representing the two-dimensional ocean, we set the end points of $\hat{\psi}$ equal to zero in both east-west- and north-south-direction. We are in other words approximating an ocean that is bounded by continents in both directions. For representing the atmosphere, we allow for periodic boundaries in east-west direction. However, we set $\hat{\psi}$ equal to zero in the north-south endpoints, which is comparable to setting the flow to zero on the Earth's poles.

Our algorithm for 2 + 1 dimensions thus becomes

```
initialise psi, zeta
for n = 0,..., T-1:
    for j = 0, ..., X:
        for i = 0, ..., Y;
            calculate zeta(i,j,n+1) using
            forward or centered
            differences scheme
    calculate psi(n+1) using
    Jacobi's method
```

where Y is the grid size in the y-direction.

D. Initial conditions

For the initial $\hat{\psi}$ we use both a sine wave and a centered Gaussian. For the 1 + 1 dimensional case, we use

$$\hat{\psi}^0 = \sin(4\pi x) \quad (32)$$

$$\hat{\zeta}^0 = -16\pi^2 \sin(4\pi x) \quad (33)$$

$\hat{\zeta}$ being the double derivative of $\hat{\psi}$, or

$$\hat{\psi}^0 = \exp\left(-\frac{(x-x_0)^2}{\sigma^2}\right) \quad (34)$$

$$\hat{\zeta}^0 = -\frac{2}{\sigma^4}\exp\left(-\frac{(x-x_0)^2}{\sigma^2}\right)\left(\sigma^2 - 2(x-x_0)^2\right) \quad (35)$$

Since we use a centered Gaussian, we have $x_0 = 0.5$. We try different values for σ around $\sigma = 0.1$.

For the 2 + 1 dimensional case we use initial conditions that depend on both x and y. However, we let the initial conditions be the product of two functions depending only on x and y respectively. Since we want the initial conditions to go zero in the boundaries for both spatial dimensions, we let both functions have the same form as in the 1 + 1 dimensional case. The result is

$$\hat{\psi}^0 = \sin(4\pi x)\sin(4\pi y) \quad (36)$$

$$\hat{\zeta}^0 = -32\pi^2 \sin(4\pi x)\sin(4\pi y) \quad (37)$$

or for the Gaussian

$$\hat{\psi}^0 = \exp\left(-\frac{(x-x_0)^2}{\sigma^2} - \frac{(y-y_0)^2}{\sigma^2}\right) \quad (38)$$

$$\hat{\zeta}^0 = -\frac{4}{\sigma^4}\exp\left(-\frac{(x-x_0)^2}{\sigma^2} - \frac{(y-y_0)^2}{\sigma^2}\right) \quad (39)$$

$$\times\left(\sigma^2 - (x-x_0)^2 - (y-y_0)^2\right) \quad (40)$$

We let $y_0 = x_0 = 0.5$, making the two-dimensional initial Gaussian a centered peak in the domain.

E. Implementation

We implement the algorithms using `C++`, and the `armadillo` library. To analyse the data we use `python 3.8.5`, with the libraries `NumPy` and `pandas`. For visualisation, we use the `python` library `matplotlib`. A comparison between our numerical results and the analytical solutions can be found in the appendix 12.

III. RESULTS

In this section we present our main findings. We begin by presenting our comparison between different time stepping methods. Thereafter, we present the different Rossby waves with one spatial dimension. Lastly we present Rossby waves in two spatial dimensions.

A. Time step method comparison

In figure 1 we see the evolvement of the sine wave in the periodic domain for FTCS scheme and the CTCS scheme, using a $\Delta t = 1$. While the amplitude of the sine wave in FTCS is increasing regularly with time, the amplitude of the CTCS scheme remains rather stable.

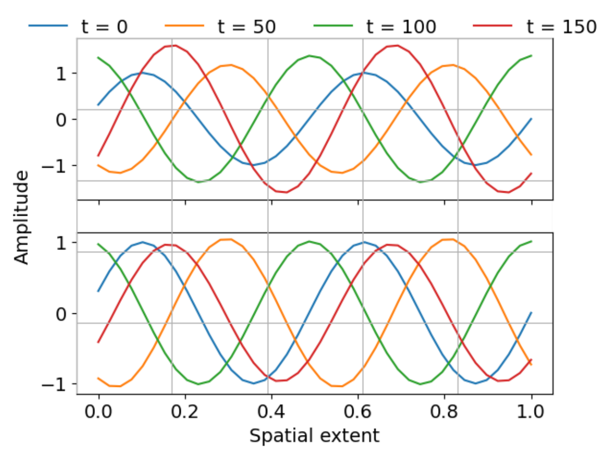

Figure 1. The streamfunction $\hat{\psi}$ in a periodic domain and initially a sine wave plotted for different times using the forward difference scheme (top) and the centered difference scheme (bottom), with $\Delta x = 1/40$ and $\Delta t = 1$.

B. 1 + 1 dimensional Rossby waves

In figure 2 we see the evolvement of the sine wave in the periodic domain over a time $T = 150$. In this and all following simulations the CTCS scheme has been used. We can find the period of the wave, or the distance in time between two wave crest in the same spatial point, to be $T = 80$. Hence, we obtain the phase speed $|c| = 0.00625$. We observe from the figure that the waves are propagating in the westward direction.

Similarly a sine wave in a bounded domain was simulated over a time $T = 150$. The resulting evolution of the model is presented in figure 3. Simulations in the periodic domain of centered Gaussian initial stream functions are presented in figure 4, 5 and 6 having $\sigma = 0.1$, 0.05 and 0.15 respectively. A centered Gaussian with $\sigma = 0.1$ was simulated in a bounded domain and is presented in figure 7.

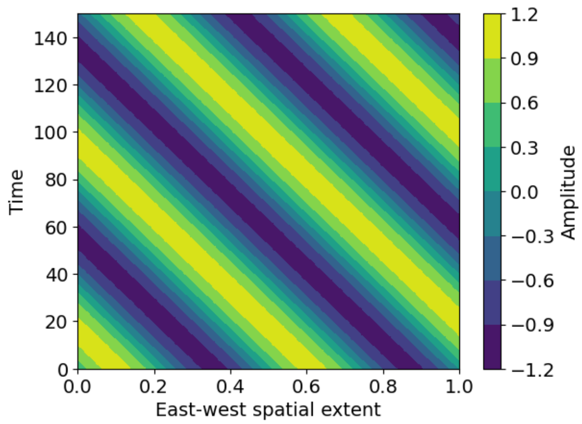

Figure 2. Hovmöller diagram for a Rossby wave initially a sine wave in a periodic domain. Here $\Delta x = 1/40$ and $\Delta t = 1/40$.

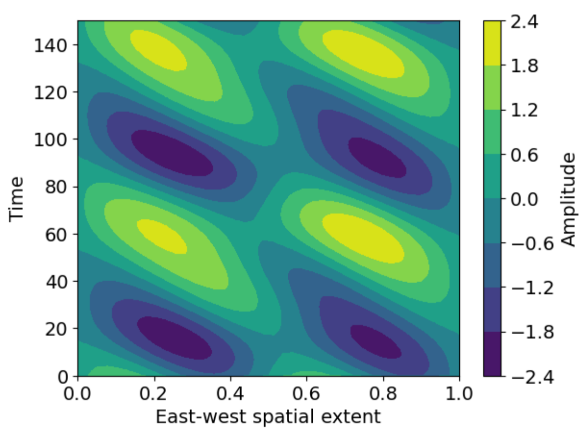

Figure 3. Hovmöller diagram for a Rossby wave initially a sine wave in a bounded domain. Here $\Delta x = 1/40$ and $\Delta t = 1/40$.

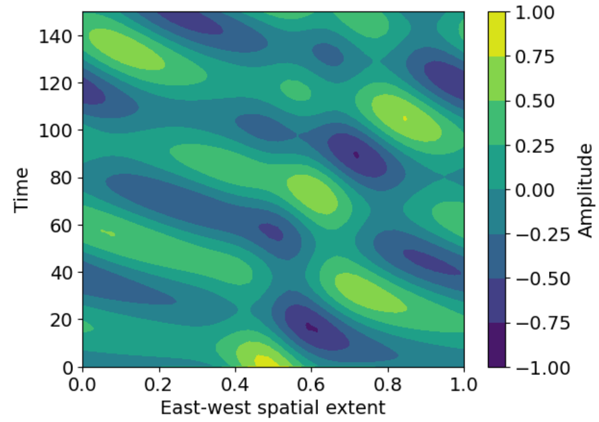

Figure 4. Hovmöller diagram for a Rossby wave initially a centered Gaussian with $\sigma = 0.1$ in a periodic domain. Here $\Delta x = 1/40$ and $\Delta t = 1/40$.

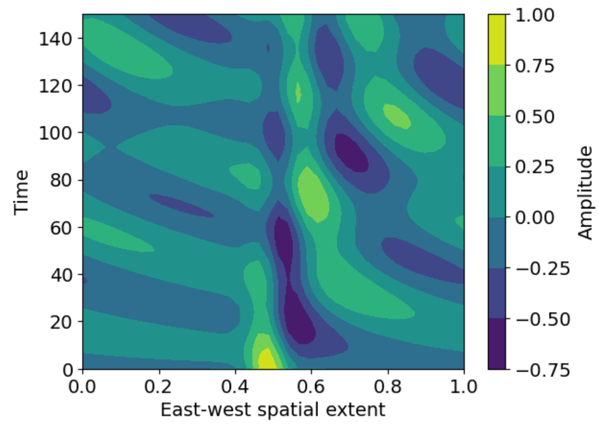

Figure 5. Hovmöller diagram for a Rossby wave initially a centered Gaussian with $\sigma = 0.05$ in a periodic domain. Here $\Delta x = 1/40$ and $\Delta t = 1/40$.

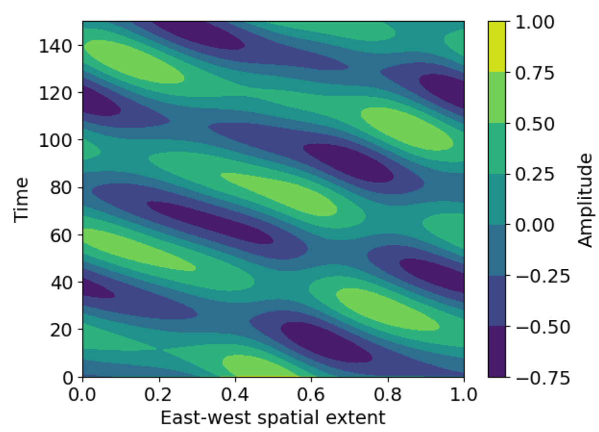

Figure 6. Hovmöller diagram for a Rossby wave initially a centered Gaussian with $\sigma = 0.15$ in a periodic domain. Here $\Delta x = 1/40$ and $\Delta t = 1/40$.

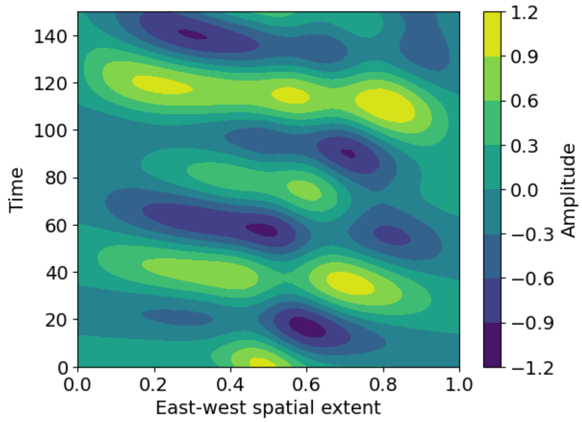

Figure 7. Hovmöller diagram for a Rossby wave initially a centered Gaussian with $\sigma = 0.1$ in a bounded domain. Here $\Delta x = 1/40$ and $\Delta t = 1/40$.

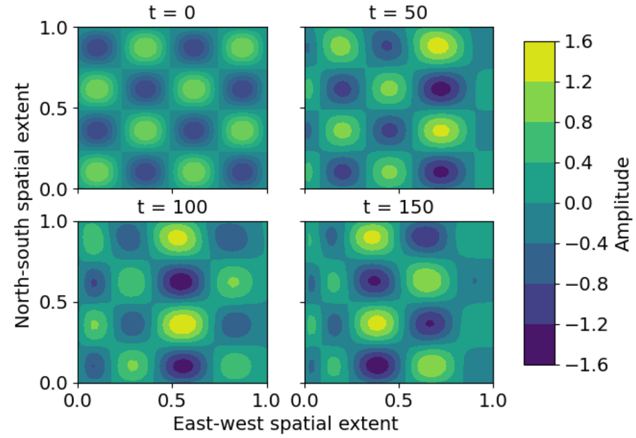

Figure 9. A Rossby wave initially a sine wave in a two-dimensional bounded domain for four different times. Here $\Delta x = \Delta y = 1/40$ and $\Delta t = 1/40$.

C. 2 + 1 dimensional Rossby waves

We simulated an initial sine wave in the semi-periodic domain and in the bounded domain. To show the temporal evolution the times $t = 0$, 50, 100 and 150 was chosen and rendered in the figures. The sine wave simulations are presented in figure 8 and 9. Simulations of centered Gaussians with $\sigma = 0.1$ in semi-periodic and bounded domains are presented in figure 10 and 11. These are both very similar, and only figure 10 is included in "Results", while figure 11 can be found in the appendix. As in the 1 + 1 dimensional case we observe a westward direction of the phase velocity.

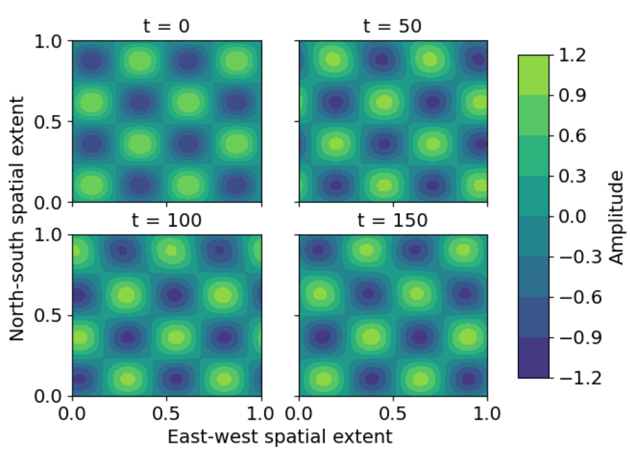

Figure 8. A Rossby wave initially a sine wave in a two-dimensional semi-periodic domain for four different times. Here $\Delta x = \Delta y = 1/40$ and $\Delta t = 1/40$.

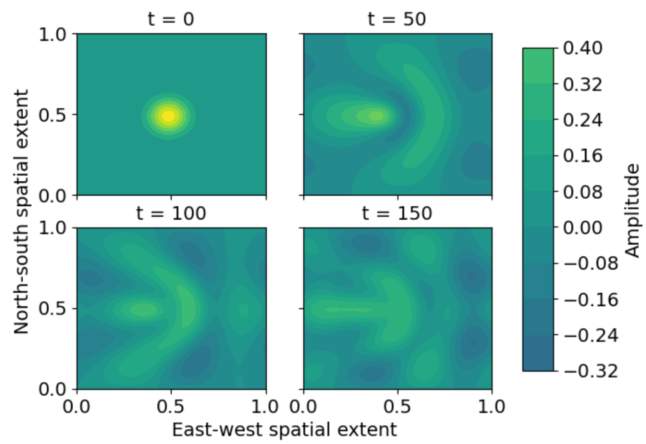

Figure 10. A Rossby wave initially a centered Gaussian with $\sigma = 0.1$ in a two-dimensional semi-periodic domain for four different times. Here $\Delta x = \Delta y = 1/40$ and $\Delta t = 1/40$.

IV. DISCUSSION

From the time-stepping routines in figure 1 we can clearly see that CTCS is a better scheme, as its amplitude remains constant throughout the time period, while the FTCS amplitude starts growing unstably. The CFL condition for the CTCS scheme is violated, as $\Delta t = 40\Delta x$, which means that it is not under stable conditions. However, we see that even such a big violation of the CFL condition has little effect on the amplitude growth in the CTCS scheme on the time scales we consider.

For the periodic sine in 1 + 1 dimensions, we can compare the phase speed $|c| = 0.00625$ we found from the Hovmöller diagram with the one from our analytical expression. Putting the same wavenumber k in our analytical solution, with $\beta = 1$, yields $|c| = 0.00633$. The numerically acquired phase speed is slightly smaller, but is rather close to the theoretical phase speed. The relative error is 0.0128.

If we consider the sine in the bounded domain in figure 3, the phase speed is less straightforward to extract. The enforcement of the Dirichlet boundary conditions are causing clear nodes and anti-nodes in the Hövmuller plot, and the wave appears more standing than travelling. This can be rationalized if we consider the form of the analytical solution the Rossby wave. This predicts that a sine wave wrapped around the moving wave should force it to be zero at the sine function's zeroes, but also that the waves will superimpose when their functions align. We can see this by the fact that the amplitude of the waves are twice that of the periodic sine.

When we consider the periodic Gaussian in figure 4 we see a pattern with greater variation in time than that of the sine wave. Due to this it is also more difficult to extract a phase speed. Still, we can see a tilted pattern indicated westward movement. This pattern is more tilted than for the sine wave, which could indicate a larger phase speed. One of the main differences between the Gaussian and the sine wave is the number of clear troughs and crest that are present at each time. For the Gaussian there are usually only two simultaneosly, and the pattern is more irregular. Adjusting the Gaussian to a smaller width, as in figure 5, leads to more spatially concentrated troughs and crest, while for the larger width in figure 6 they become more spread out. The phase speed does not appear to be affected, as the "tilt" in the wave pattern seems to be the same.

The Gaussian in the bounded domain in figure 7 has a pattern more similar to that of the bounded sine in that it alternates between clear maxima and minima in a way that appear almost as a standing wave. While we begin with only an initial centered peak, this evolves to two peaks at $t = 40$, which has evolved to three peaks at $t = 120$. There is in other words more evolvement of the wave pattern in time for the Gaussian than for the sine wave. However, we also note that apart from having more defined throughs and crest, the pattern in 7 is not so different from that of 4.

Finally, we turn to the two-dimensional waves. The results appear rather similar for the bounded and periodic boundaries with the respective initial conditions, especially for the Gaussians in figures 10 and 11. This might be because the waves are initiated with a centered peak far away from the boundaries, which might not lead to much interaction with the boundaries over the time we are looking at. However, we also recall from the one-dimensional case that the bounded and periodic Gaussian were not too different in patterns. It can be debated how realistic the initial condition for the Gaussian is, but it could perhaps be compared to a high pressure in the ocean or atmosphere. For the sine waves in figure 8 and 9 we see a difference between the boundary conditions in that while the form of the periodic waves remains relatively unchanged throughout their movement, the bounded sine waves seems to be stretched out on the east side and squeezed together in the west. This is likely due to the western propagation of the waves. The sine waves are quite homogeneous in the y-direction. This implies that a one dimensional solution might not be such a bad representation after all.

V. CONCLUSION

In summary, we developed and implemented numerical methods to simulate Rossby waves in both 1 + 1 and 2 + 1 dimensions. We used both sine wave and centered Gaussian functions for the initial stream functions in our simulations and studied their behavior in both the periodic and bounded domains. We found that the CTCS scheme yielded stable results for our model with the condition being that the time step must be smaller or equal to the spatial step length, $\Delta t \leq \Delta x$. We observed that the simulations showed the expected behavior by propagating in the westward direction. From the simulation of an initial sine wave in a periodic domain we obtained an approximate phase speed of $|c| \simeq 0.00625$, with a relative error of 0.0128 to the analytical result. Our results indicate that the behavior of the Rossby waves in 2 spatial dimensions is also found in the 1 dimensional case, hence, simulating in 1 dimension could in some cases be a sufficient approximation.

To further illustrate the Rossby wave's behavior, we should simulate over much longer time periods. This would also further illustrate the stability of our model. Additionally, the class we developed for this project could be expanded or applied to other wave problems. One task could be to create more realistic domains and account for waves resulting from linearised topography.

[1] Aslam Abdullah. Simplified von neumann stability analysis of wave equation numerical solution. *ARPN Journal of Engineering and Applied Sciences*, 14(24), 12 2019.

[2] Erlend Andreas Longva; Astrid Bragstad Gjelsvik. Numerical studies of phase transitions in magnetic systems using an ising model. GitHub link, 2020.

[3] Erlend Andreas Longva; Astrid Bragstad Gjelsvik. Solving a second order differential equation using tridiagonal matrix algorithms. GitHub link, 2020.

[4] Morten Hjort-Jensen. *Computational Physics: Lecture Notes Fall 2015*, pages 308–309. UiO, 2015.

[5] Morten Hjort-Jensen. *Computational Physics: Lecture Notes Fall 2015*, pages 319–320. UiO, 2015.

[6] Joseph Henry Lacasce. *Atmosphere-Ocean Dynamics*, pages 117–119. UiO, 2020.

[7] Joseph Henry Lacasce. *Atmosphere-Ocean Dynamics*, pages 65–66. UiO, 2020.

[8] National Ocean and Atmospheric Administration. What is a Rossby wave?, 2020. Link.
[9] Lars Petter Røed. *Atmospheres and Oceans on Computers*, pages 78–81. Springer, 2018.
[10] Yngve Nilsen. Carl Gustaf Rossby, 2011. Store norske leksikon.

Appendix A: Calculations

1. Analytical solution to Rossby waves with solid boundaries

We first calculate the terms of the equation (12) separately.

$$\frac{\partial}{\partial x}A(x)\cos(kx-\omega t) = -A(x)k\sin(kx-\omega t) + \frac{\partial A}{\partial x}\cos(kx-\omega t) \tag{A1}$$

$$\frac{\partial^2}{\partial x^2}A(x)\cos(kx-\omega t) = \frac{\partial}{\partial x}\left(-A(x)k\sin(kx-\omega t) + \frac{\partial A}{\partial x}\cos(kx-\omega t)\right) \tag{A2}$$

$$= \left(\frac{\partial^2 A}{\partial x^2} - A(x)k^2\right)\cos(kx-\omega t) - 2k\frac{\partial A}{\partial x}\sin(kx-\omega t) \tag{A3}$$

$$\frac{\partial}{\partial t}\frac{\partial^2}{\partial x^2}A(x)\cos(kx-\omega t) = \frac{\partial}{\partial t}\left(\left(\frac{\partial^2 A}{\partial x^2} - A(x)k^2\right)\cos(kx-\omega t) - 2k\frac{\partial A}{\partial x}\sin(kx-\omega t)\right) \tag{A4}$$

$$= \omega\left(\frac{\partial^2 A}{\partial x^2} - A(x)k^2\right)\sin(kx-\omega t) + 2\omega k\frac{\partial A}{\partial x}\cos(kx-\omega t) \tag{A5}$$

We then calculate equation (12).

$$\frac{\partial}{\partial t}\frac{\partial^2}{\partial x^2}A(x)\cos(kx-\omega t) + \beta\frac{\partial}{\partial x}A(x)\cos(kx-\omega t) = 0 \tag{A6}$$

$$\omega\left(\frac{\partial^2 A}{\partial x^2} - A(x)k^2\right)\sin(kx-\omega t) + 2\omega k\frac{\partial A}{\partial x}\cos(kx-\omega t) + \beta\left(-A(x)k\sin(kx-\omega t) + \frac{\partial A}{\partial x}\cos(kx-\omega t)\right) = 0 \tag{A7}$$

$$\frac{\partial A}{\partial x}(2\omega k+\beta)\cos(kx-\omega t) + \left(\omega\frac{\partial^2 A}{\partial x^2} - A(x)\left(\omega k^2+\beta k\right)\right)\sin(kx-\omega t) = 0 \tag{A8}$$

We set both all the cosine terms and the sine terms equal to zero separately. We can then calculate the dispersion relation and the differential equation for $A(x)$.

$$\frac{\partial A}{\partial x}(2\omega k+\beta) = 0 \tag{A9}$$

$$2\omega k+\beta = 0 \tag{A10}$$

$$\omega = -\frac{\beta}{2k} \tag{A11}$$

$$\omega\frac{\partial^2 A}{\partial x^2} - \left(\omega k^2+\beta k\right)A(x) = 0 \tag{A12}$$

$$-\frac{\beta}{2k}\frac{\partial^2 A}{\partial x^2} - \left(-\frac{\beta}{2k}k^2+\beta k\right)A(x) = 0 \tag{A13}$$

$$-\frac{\beta}{2k}\left(\frac{\partial^2 A}{\partial x^2} + k^2 A(x)\right) = 0 \tag{A14}$$

Appendix B: Figures

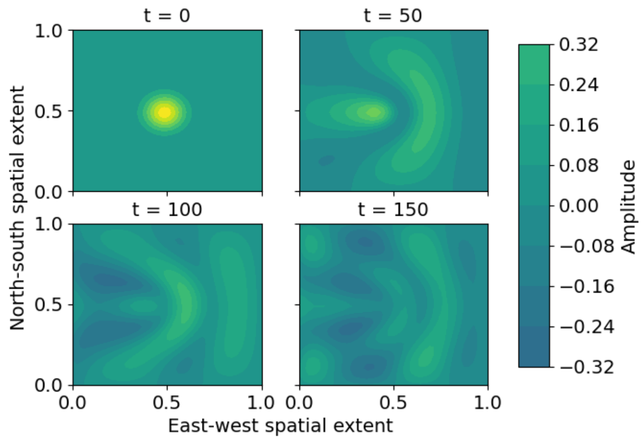

Figure 11. A Rossby wave initially a centered Gaussian with $\sigma = 0.1$ in a two-dimensional bounded domain for four different times. Here $\Delta x = \Delta y = 1/40$ and $\Delta t = 1/40$.

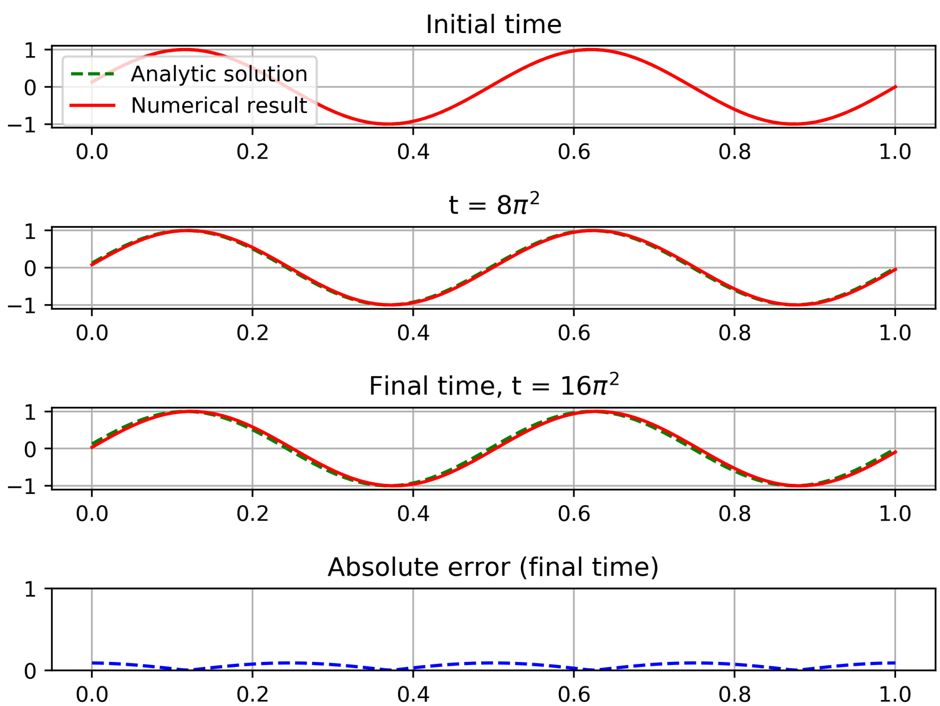

Figure 12. Comparison of analytic wave solution with numerical results in 1 + 1 dimensions using periodic boundary conditions. For times $t = 0$, $8\pi^2$ and $16\pi^2$. Here $\Delta x = 1/100$ and $\Delta t = 1/100$.